Supporting information

$KVPO_4F$ as a novel insertion-type anode for potassium ion batteries

Hong Tan, Xiaoqiong Du, Jian-Qiu Huang, Biao Zhang *
Department of Applied Physics, the Hong Kong Polytechnic University, Hung Hom, Hong Kong, P.R.
Corresponding author: Biao Zhang. Email: biao.ap.zhang@polyu.edu.hk

Experimental

1. $KVPO_4F$ preparation

$KVPO_4F$ was prepared by a sol-gel method. For a typical synthesis, 0.92 g $NH_4H_2PO_4$, 0.936 g H_4NO_3V, 0.557 g KF and 1.228 g citric acid were first dissolved in 30 ml deionized water by sequence in a 50 ml beaker with stirring. After evaporating the water under continuous stirring at 80 ℃, the obtained mixture was transferred to a vacuum oven at 60 ℃ overnight. Prior to thermal treatment, the dried mixture was finely ground into powder in an agate mortar. The green-colored powder was then annealed in a tube furnace at 700 ℃ for 8 h under Ar protection. The obtained black powder was directly used for the subsequent characterization and electrochemical test without further treatment.

2. Material Characterization

The phase was determined by X-ray diffraction (XRD) performing on a Rigaku Smart Lab 9kW diffractometer using Cu-Kα radiation (λ=1.54178Å). The morphology of the sample was characterized by scanning electron microscopy (TESCAN MAIA3) and transmission electron microscopy (JEOL Model JEM-2100F).

3. Electrochemical test

For the fabrication of $KVPO_4F$ electrode, 70 wt% $KVPO_4F$, 20 wt% carbon black and 10 wt% Polyvinylidene fluoride (PVDF) were first dry-mixed in an agate mortar and then wet-mixed with N-Methyl-2-pyrrolidone (NMP) to form a homogeneous slurry.

The obtained slurry was cast onto a copper foil and dried in an oven at 60 ℃ overnight. Discs with a diameter of 12 mm were cut from the dried tape to employ as the anodes for half-cell assembly while potassium plate was used as counter electrode. To examine the performance of $KVPO_4F$ as cathode, aluminum foil, instead of copper foil, was used to prepare the electrodes. For in-situ XRD test, the aforementioned electrode slurry was cast on a Be window. The typical loading of $KVPO_4F$ is around 2 mg for each electrode. 1 M KPF_6 in ethylene carbonate (EC)/propylene carbonate (PC) (1:1 in volume) was used as electrolyte and the glass fiber (Whatman, GF/D) was employed as a separator. The half-cell was assembled in a standard CR2032 coin cell configuration and the symmetric $KVPO_4F$ full cell was assembled in a two-electrode Swagelok cell. Typically, for the fabrication of symmetric $KVPO_4F$ full cells, the active mass ratio of cathode versus anode is maintained at around 2:1. All assembly was carried out in an argon-filled glove box with O_2 and H_2O content less than 0.5 ppm. For the XRD characterization of the electrode after cycles, the cell was disassembled in glove box and the electrode was washed with DMC for several times before it was sealed in an in-situ XRD holder with a beryllium window. The galvanostatic tests were performed on LAND CT2001A Battery Testing systems. Cyclic voltammetry (CV) tests were conducted on a Solartron Analytical 1400 electrochemical workstation.

Supporting figures and tables

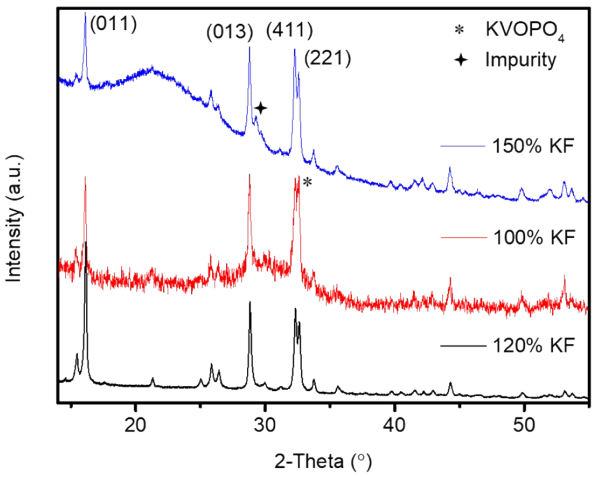

Figure S1. XRD patterns of the samples prepared with various KF content (100%, 120% and 150%) based on the stoichiometric composition of $KVPO_4F$. The high peak intensity at 32.6 degree indicates the presence of $KVOPO_4$.[1]

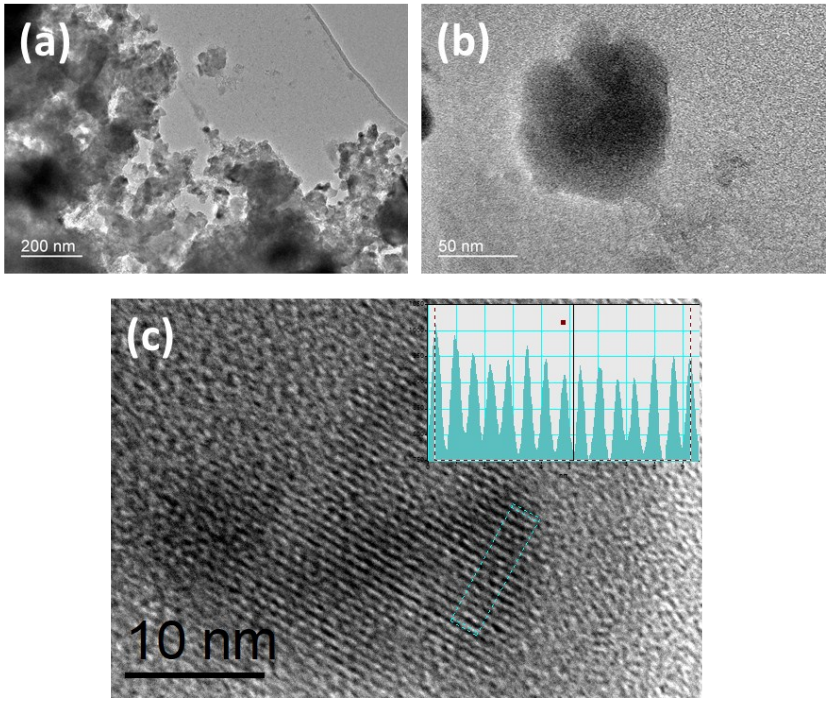

Figure S2. (a), (b) TEM images of as-obtained $KVPO_4F$ and (c) high-magnification TEM image showing an interlayer spacing of 6.42 Å, indexed to the (200) plane.

The Rietveld refinement results including parameters and crystallographic data of the as-prepared $KVPO_4F$ is shown in Table S1. The CIF profile proposed by Fedotov et al[2] was used as a starting structure model for the refinement.

Table S1. Rietveld refinement results of the obtained $KVPO_4F$

		$KVPO_4F$	**Space group $Pna2_1$**			
	a=12.8289 Å	b=6.4046 Å	c=10.6038 Å	z=8		V=871.26 Å^3
Atom	Position	x/a	y/b	z/c	Occ	B_{iso}
K1	4a	0.3705(5)	0.778(1)	0.290(5)	0.5	1.8(1)
K1’	4a	0.3876(6)	0.778(3)	0.321(3)	0.5	1.8(1)
K2	4a	0.1075(5)	0.719(2)	0.043(2)	0.5	1.8(1)
K2’	4a	0.0937(3)	0.679(1)	0.0728(12)	0.5	1.8(1)
V1	4a	0.3831(3)	0.4915(3)	0	1	0.75(5)
V2	4a	0.2478(3)	0.2535(3)	0.2489(10)	1	0.75(5)
P1	4a	0.502(4)	0.333(3)	0.257(3)	1	0.75(5)
P2	4a	0.1819(12)	0.4968(9)	0.4935(9)	1	0.75(5)
O1	4a	0.486(2)	0.479(1)	0.143(2)	1	1.0(1)
O2	4a	0.519(2)	0.479(4)	0.372(1)	1	1.0(1)
O3	4a	0.401(2)	0.212(3)	0.290(9)	1	1.0(1)
O4	4a	0.592(7)	0.207(7)	0.229(10)	1	1.0(1)
O5	4a	0.118(3)	0.312(6)	0.532(4)	1	1.0(1)
O6	4a	0.108(3)	0.673(6)	0.467(5)	1	1.0(1)
O7	4a	0.242(3)	0.537(7)	0.629(7)	1	1.0(1)
O8	4a	0.250(3)	0.462(3)	0.391(6)	1	1.0(1)
F1	4a	0.272(1)	0.524(2)	0.867(10)	1	1.0(1)
F2	4a	0.272(2)	0.483(1)	0.121(4)	1	1.0(1)

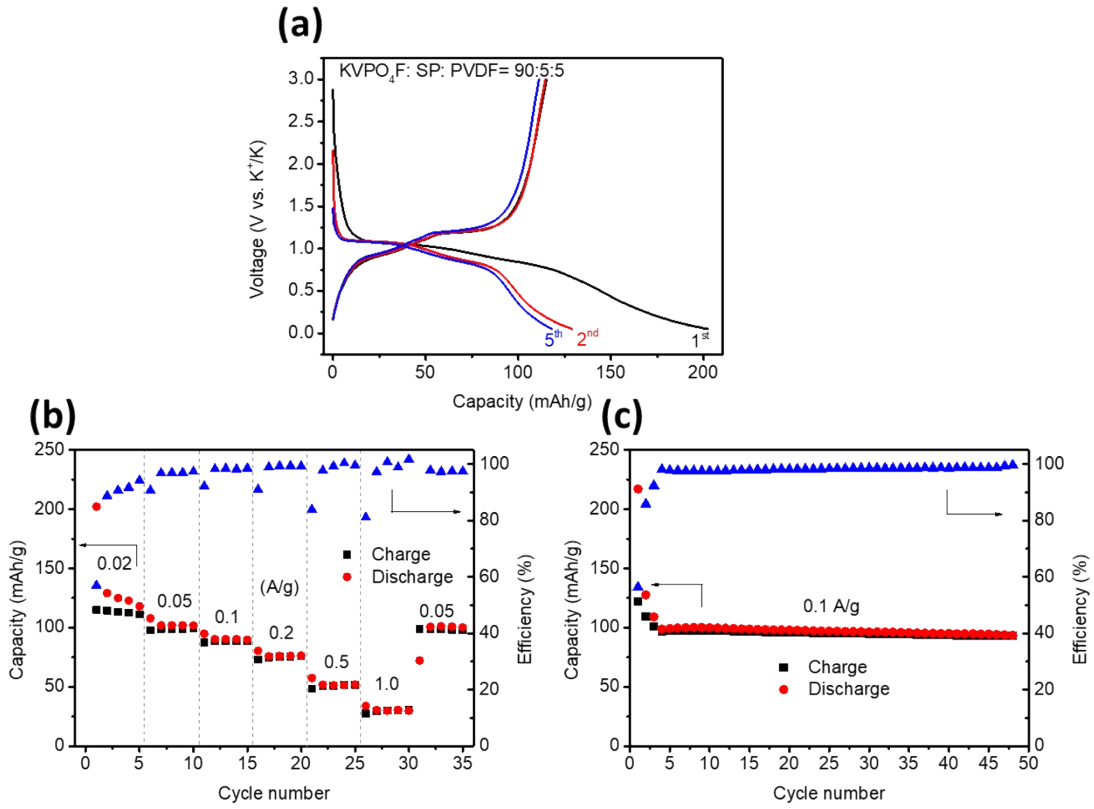

Figure S3. (a) Voltage profiles (b) Rate capability and (c) Cyclic performance of electrodes with 90 wt.% $KVPO_4F$.

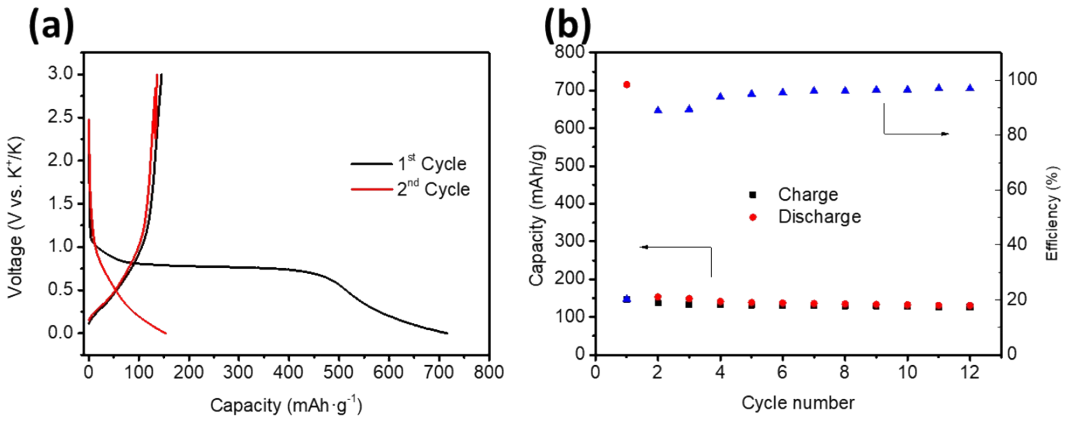

Figure S4. (a) Voltage profiles of the 1st and 2nd cycle and (b) cycling test of pure carbon black as anode for K-ion half-cell.

The GITT test was carried out to evaluate the diffusion coefficient of $KVPO_4F$ at 25 ℃. The discharge/charge duration time is set as 30 min while the rest interval is set as 2 h. The calculation of the diffusion coefficient was based on previous work.[3] As shown in equation (1), m_B is the mass of active material of electrode, M_B is the molar mass of $KVPO_4F$, V_M is the molar volume of $KVPO_4F$, the theoretical density ρ of $KVPO_4F$ was calculated based on the crystallographic data obtained by refinement following Rachel Rosten's method.[4] S is the geometric area of the electrode, the value of which is 1.13 cm^2 in this case, τ is the duration time upon each charge/discharge.

$$D = \frac{4}{\pi\tau}\left(\frac{m_B V_M}{M_B S}\right)^2\left(\frac{\Delta E_s}{\Delta E_\tau}\right)^2 \qquad \text{—— (1)}$$

The diffusion coefficients deduced from the GITT profiles and equation (1) are depicted in Fig. S5.

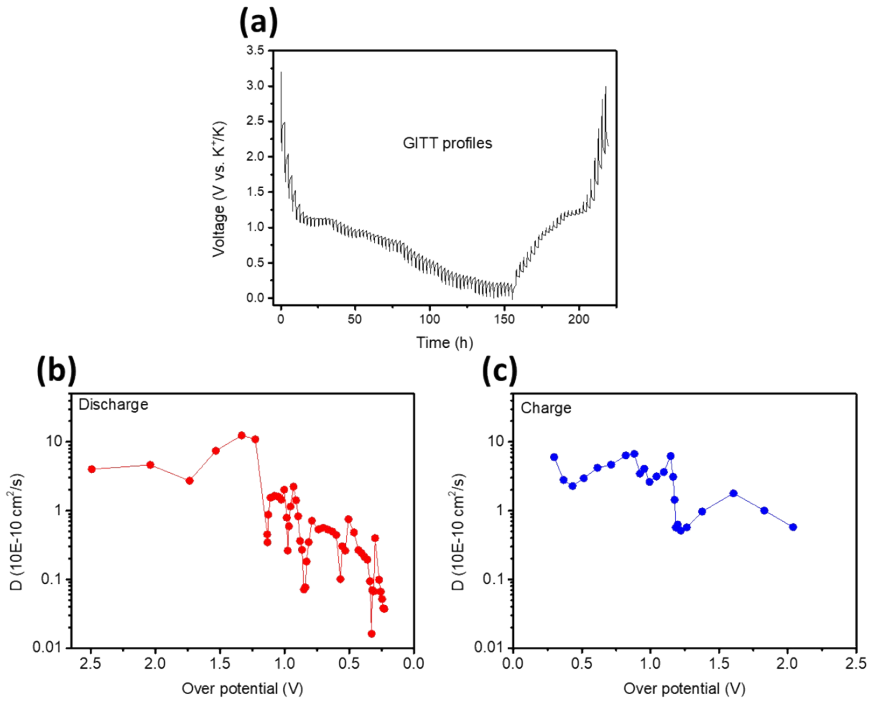

Figure S5. (a) GITT profiles of $KVPO_4F$ and the diffusion coefficients deduced from the GITT profiles as a function of the cell potential upon (b) discharge and (c) charge.

Table S2. Comparison of the performance of insertion type anode and graphite for K-ion batteries

Insertion type anode	Reversible capacity	Capacity retention	Rate capability	Electrolyte	Loading	Reference
$K_2Ti_6O_{13}$	90 $mAh \cdot g^{-1}$ at 50 $mA \cdot g^{-1}$	84 % after 1000 cycles at 500 $mA \cdot g^{-1}$	57 $mAh \cdot g^{-1}$ at 1000 $mA \cdot g^{-1}$	0.8 $mol \cdot L^{-1}$ KPF_6 in PC/FEC (5%)	-	5
$K_2Ti_4O_9$	80 $mAh \cdot g^{-1}$ at 100 $mA \cdot g^{-1}$	50 % after 30 cycles at 100 $mA \cdot g^{-1}$	20 $mAh \cdot g^{-1}$ at 2000 $mA \cdot g^{-1}$	1 $mol \cdot L^{-1}$ KPF_6 in EC/PC(1:1)	2.0 - 3.0 $mg \cdot cm^{-2}$	6
$K_2Ti_8O_{17}$	181 $mAh \cdot g^{-1}$ at 20 $mA \cdot g^{-1}$	61 % after 50 cycles at 20 $mA \cdot g^{-1}$	44.2 $mAh \cdot g^{-1}$ at 500 $mA \cdot g^{-1}$	0.8 $mol \cdot L^{-1}$ KPF_6 in EC/DEC(1:1)	-	7
$KTi_2(PO_4)_3$	75.6 $mAh \cdot g^{-1}$ at 64 $mA \cdot g^{-1}$	~95 % after 100 cycles at 64 $mA \cdot g^{-1}$	65 $mAh \cdot g^{-1}$ at 640 $mA \cdot g^{-1}$	0.8 $mol \cdot L^{-1}$ KPF_6 in EC/DEC(1:1)	1.0 $mg \cdot cm^{-2}$	8
MoS_2	73 $mAh \cdot g^{-1}$ at 10 $mA \cdot g^{-1}$	97.5 % after 200 cycles at 10 $mA \cdot g^{-1}$	55 $mAh \cdot g^{-1}$ at 160 $mA \cdot g^{-1}$	60 uL 0.5$mol \cdot L^{-1}$ KPF_6 in EC/PC(1:1)	2.0 $mg \cdot cm^{-2}$	9
Graphite	263 $mAh \cdot g^{-1}$ at 28 $mA \cdot g^{-1}$	50 % after 50 cycles at 140 $mA \cdot g^{-1}$	80 $mAh \cdot g^{-1}$ at 279 $mA \cdot g^{-1}$	0.8 $mol \cdot L^{-1}$ KPF_6 in EC/DEC(1:1)	2.0 $mg \cdot cm^{-2}$	10
$KVPO_4F$	150 $mAh \cdot g^{-1}$ at 20 $mA \cdot g^{-1}$	91 % after 100 cycles at 100 $mA \cdot g^{-1}$	65 $mAh \cdot g^{-1}$ at 2000 $mA \cdot g^{-1}$	80 uL 1 $mol \cdot L^{-1}$ KPF_6 in EC/PC(1:1)	2.0 $mg \cdot cm^{-2}$	This work
	127 $mAh \cdot g^{-1}$ at 50 $mA \cdot g^{-1}$	95 % after rate test at 50 $mA \cdot g^{-1}$	60 $mAh \cdot g^{-1}$ at 1000 $mA \cdot g^{-1}$	80 uL 1 $mol \cdot L^{-1}$ KPF_6 in EC/PC(1:1)	4.0 $mg \cdot cm^{-2}$	

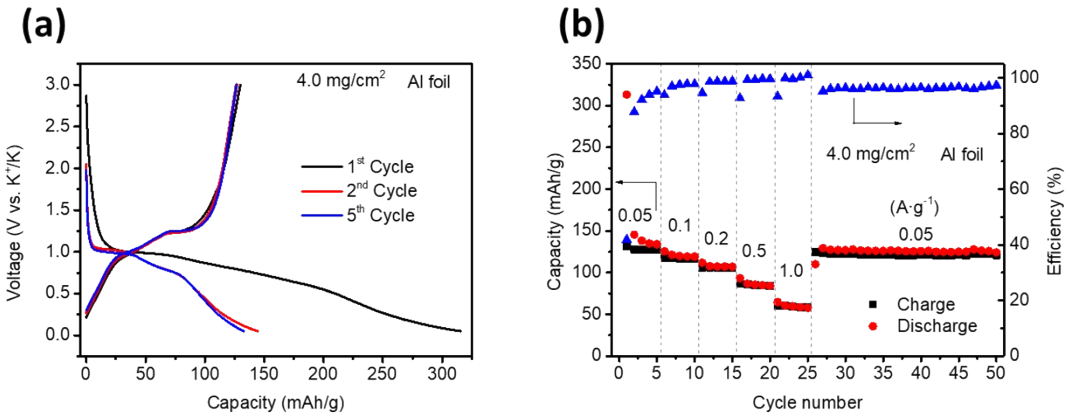

Figure S6. (a) Voltage profiles and (b) Rate performance of electrodes using aluminum foil as a current collector and with a higher mass loading of active material (4.0 mg/cm^2).

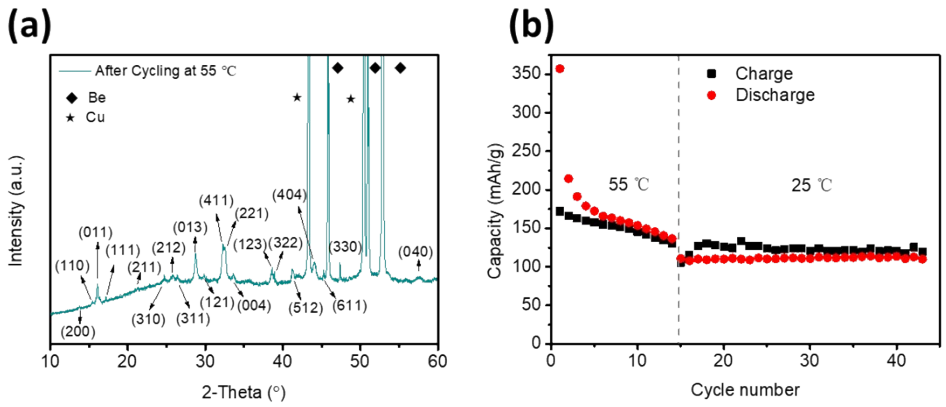

Figure S7. (a) XRD patterns of the electrode after 50 cycles at 55 ℃; (b) Cycling performance of the $KVPO_4F$ electrode transferring from 55 ℃ to 25 ℃.

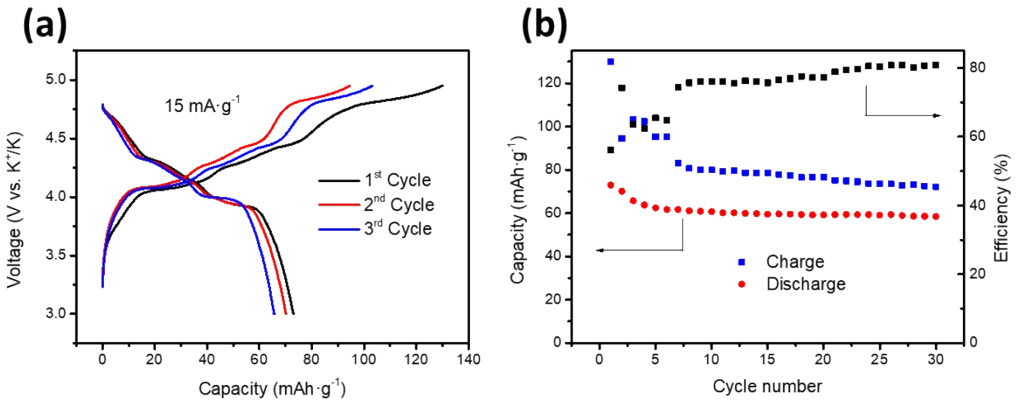

Figure S8. (a) The voltage profiles of the as-prepared $KVPO_4F$ as cathode for K-ion half-cell within 3.0 - 4.95 V (vs. K^+/K) and the corresponding (b) Cycling performance.

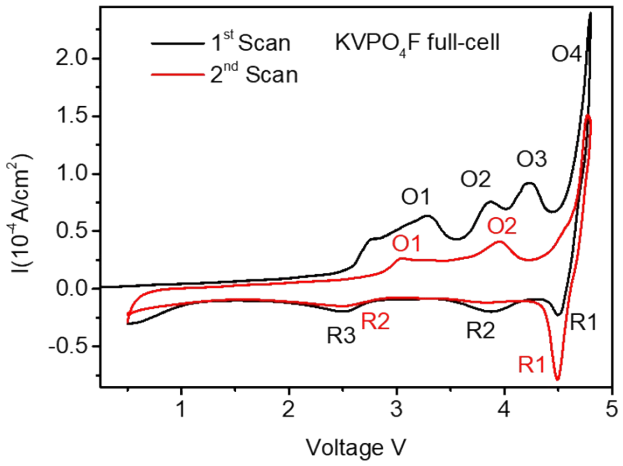

Figure S9. The CV curves of the symmetric $KVPO_4F$ full cell with the oxidation peaks referring to the structure evolution from $KVPO_4F$ to $K_{0.75}VPO_4F$ (O1), $K_{0.625}VPO_4F$ (O2), $K_{0.5}VPO_4F$ (O3) and VPO_4F (O4), as suggested by Ceder et al[11].

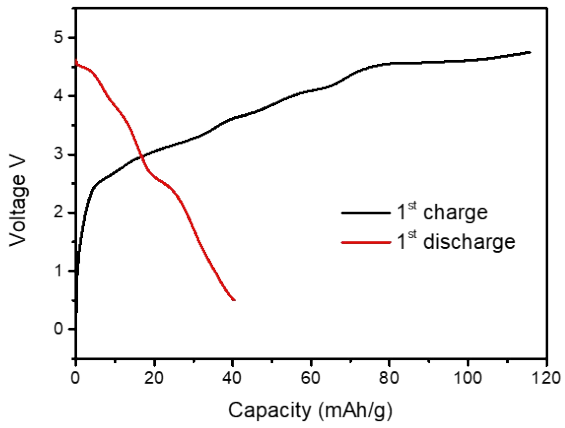

Figure S10. The voltage profiles of the 1st cycle for the symmetric $KVPO_4F$ full cell.

References

1 K. Chihara, A. Katogi, K. Kubota and S. Komaba, *Chem. Commun.*, 2017, **53**, 5208-5211.

2 S. S. Fedotov, N. R. Khasanova, A. S. Samarin, O. A. Drozhzhin, D. Batuk, O. M. Karakulina, J. Hadermann, A. M. Abakumov and E. V. Antipov, *Chem. Mater.*, 2016, **28**, 411-415.

3 Z. Jian, Z. Xing, C. Bommier, Z. Li and X. Ji, *Adv. Energy Mater.*, 2016, **6**, 1-5.

4 R. Rosten, M. Koski and E. Koppana, *J. Undergrad. Mater. Res.*, 2018, **2**, 1-4.

5 S. Dong, Z. Li, Z. Xing, X. Wu, X. Ji and X. Zhang, *ACS Appl. Mater. Interfaces*, 2018, **10**, 15542-15547.

6 B. Kishore, V. G and N. Munichandraiah, *J. Electrochem. Soc.*, 2016, **163**, A2551-A2554.

7 J. Han, M. Xu, Y. Niu, G. N. Li, M. Wang, Y. Zhang, M. Jia and C. M. Li, *Chem. Commun.*, 2016, **52**, 11274-11276.

8 J. Han, Y. Niu, S. Bao, Y.-N. Yu, S.-Y. Lu and M. Xu, *Chem. Commun.*, 2016, **52**, 11661-11664.

9 X. Ren, Q. Zhao, W. D. McCulloch and Y. Wu, *Nano Res.*, 2017, **10**, 1313-1321.

10 Z. Jian, W. Luo and X. Ji, *J. Am. Chem. Soc.*, 2015, **137**, 11566-11569.

11 H. Kim, D. Seo, M. Bianchini, R. J. Clément, H. Kim, J. C. Kim, Y. Tian, T. Shi, W. Yoon and G. Ceder, *Adv. Energy Mater.*, 2018, **8**, 1801591.